e-ISSN 2083–4640
ISSN 1507–1367

RESEARCH PAPER

Reports of Practical Oncology and Radiotherapy
2025, Volume 30, Number 1, pages: 79–87
DOI: 10.5603/rpor.104733
Submitted: 22.07.2024
Accepted: 30.01.2025

Investigation of the beam width and profile of kilovoltage CBCT using different measurement techniques and analysis of the dosimetric effects of beam parameters

Szilvia Gazdag-Hegyesi[1, 2], Ádám Gáldi[1, 3], Enikő Koszta[1], Gábor Stelczer[1, 4], Domonkos Szegedi[1, 2], Tibor Major[1, 5, 6], Csilla Pesznyák[1, 4]

[1]Center of Radiotherapy, National Institute of Oncology, Budapest, Hungary
[2]Doctoral School of Physical Sciences, Budapest University of Technology and Economics, Budapest, Hungary
[3]Doctoral School, Semmelweis University, Budapest, Hungary
[4]Institute of Nuclear Techniques, Budapest University of Technology and Economics, Budapest, Hungary
[5]Department of Oncology, Semmelweis University, Budapest, Hungary
[6]Department of Molecular Immunology and Toxicology and the National Tumor Biology Laboratory, National Institute of Oncology, Budapest, Hungary

ABSTRACT

Background: The aim of this study is to investigate the beam width and beam profile of kilovoltage cone beam computed tomography (kV CBCT) using different measurement techniques on an O-ring linear accelerator. The effect of the imaging beam on the dosimetric parameters was analysed.

Materials and methods: The uncertainty of field size adjustment, the dependence of beam width on field size, and the effect of deflection from the isocenter on the beam profile were investigated by ionization chamber detector matrices. The 2D beam profile of the CBCT was analysed by relative ionization chamber measurements.

Results: The average setup uncertainties of the field sizes were 0.3 mm ± 0.02 mm. The dependence of beam width on field size investigation revealed that the largest discrepancies occurred for small field sizes, which are important in determining computed tomography dose index (CTDI) values of the kV CBCT. The beam width deviation between measured and vendor-based data was larger than 1 mm below 40 mm field of view. The pelvis protocol demonstrated the smallest CTDI value difference of 2.3%, yet presented the largest effective dose deviation of 0.12 mSv.

Conclusions: The measured CTDI coefficients were higher than predicted by the manufacturer for all cases. The currently internationally recommended CTDI measurement protocols for CBCT contain no reference to the determination of the beam width as a basic element of the calculations. Based on our measurement results, the beam width parameters affect CTDI: therefore, it would be advisable to apply this type of correction.

Keywords: cone-beam CT; radiation dosimetry; CT dose index; dose length product; radiotherapy

Rep Pract Oncol Radiother 2025;30(1):79–87

Address for correspondence: Szilvia Gazdag-Hegyesi, Center of Radiotherapy, National Institute of Oncology, Hungary; e-mail: hegyesi.szilvia@oncol.hu

Introduction

The additional dose of cone-beam CT (CBCT) is lower compared to conventional diagnostic or planning CT scanning acquisition doses and therapeutic doses, therefore it has been considered negligible [1]. The development and widespread use of imaging has contributed to the reduction of CTV-PTV margins, thus reducing the dose of organs at risk [2–4].

The radiation doses of CBCT are not negligible in the case of image-guided radiotherapy (IGRT) and kilovoltage imaging based online adaptive therapy. On Halcyon or Ethos linear accelerator (Varian, Palo Alto, CA, USA) a kilovoltage (kV) cone beam imaging device is mounted perpendicular to the megavoltage (MV) source [5, 6]. Due to the ring geometry of the linear accelerator, it is not possible to build an independent laser system for patient positioning. Therefore, daily kV CBCT monitoring is mandatory for all treatment fractions in the Ethos system [7].

The additional dose caused by image-guided radiation therapy (IGRT) is particularly important in all types of IMRT techniques, in terms of late side effects or the development of secondary tumours associated with cumulative dose exposure [8, 9].

With the availability of online adaptive therapy, the number of fractional imaging sessions has increased. If online adaptive therapy is used, up to three CBCT images per fraction are required. One image is acquired for planning, one after planning before irradiation and one post-irradiation for the first five fractions, for the following treatments at least two CBCTs are necessary [10, 11].

The dose of imaging depends on the specification of the device, the size of the patient and the examined area besides the imaging protocol used [12]. During the acquisition, the aim is to achieve the best possible image quality with the lowest possible dose exposure, which is consistent with the optimization principle of radiation protection [13, 14]. Nevertheless, it is important to define exact doses in order to ascertain the overall dosage from imaging and to evaluate the associated cancer risk in image-guided radiotherapy [15].

One of the most important factors in the determination of computed tomography dose index (CTDI) is the beam width. It is not evident which parameter represents the beam width for a Varian system. During the imaging, the field of view (FOV) and the diameter of the reconstructed image (Range) parameters are combined and both can be modified. In relation to imaging protocols, the FOV parameter can take values between 10 and 280 mm, with the corresponding Range always being smaller, between 9 and 245 mm (Fig. 1). It is unclear which beam width parameter is used by the manufacturer in the determination of the CTDI and dose length product (DLP) parameters. A review of the international literature revealed no sources describing the manufacturer's measurement procedure during the commissioning of linear accelerators.

The effect of the half-bowtie filter on the shape of the beam was also investigated. The filter, placed downstream of the kilovoltage source, selectively attenuates the photons emitted from the X-ray source as a function of the radiation angle [16]. By compensating for the range of dynamic signals that reach the detector through different thicknesses of the patient's body, the bowtie helps to improve image quality by allowing a more detailed quantization of information [17].

The aim of this study is to investigate the imaging beam of kV CBCT using different measurement techniques and analysing the effects of beam properties on dosimetric parameters for different imaging protocols available for the Ethos linear accelerator.

Materials and methods

Beam width

In our study we investigated the two Ranges for each FOV value given by the Ethos software described in the introduction. Moreover, the uncertainty of the field width adjustment was determined. We also examined the dependence of beam width on field size and imaging protocol. Ionisation detection matrices were used to perform the measurements, which were placed in parallel on the table of the linear accelerator during the CBCT rotation. Since the length of the projection summation image is exactly the same as the length of the beam width, the measurements could be made with the ionisation chamber detector matrix without tracking the CBCT rotation. The IBA Matrixx Resolution (IBA Dosimetry GmbH, Gewerbegebiet Frauenholz, Schwarzenbruck, Germany) ionisation chamber detector matrix was used with a spatial resolution of

6.5 mm and an active surface area of 2530 × 2530 mm^2. The measurements were evaluated in the IBA myQA software. Another independent dosimetric system was used to validate our results. For this purpose, the PTW Octavius 1000 SRS (PTW-Freiburg, Freiburg im Breisgau, Germany) ionisation chamber detector array was applied with a resolution of 2.5 mm. The maximum active area of the PTW Octavius 1000 SRS dosimeter was 1100 × 1100 mm^2, and to avoid detector edge uncertainties, measurements were performed at a maximum field size of 80 mm. To evaluate these measurements, the PTW Mephysto dosimetry software was used. Small beam widths were measured using PTW, while beam widths exceeding 80 mm *FOV* were measured using just the IBA ionization chamber detector matrix.

In order to increase the resolution of the measurements, film dosimetry method was applied, but the sensitivity of the radiochromic film was not feasible for the energy range of the kV CBCT. Neither film dosimetry devices designed for linear accelerators, which are capable of absorbing a much higher dose and higher energy, nor conventional scanning devices, which are capable of achieving lower acquisition doses, can be used. Several measurement set-ups were applied using Fuji Medical X-ray Film Super RX-N conventional X-ray and Gafchromic EBT3 radiochromic films. The measurements with films of radiology were performed in a number of different scenarios, including with and without an X-ray cassette, with and without an intensifying filter, with the film enclosed in a black envelope, in a solid water phantom, and in free air. Imaging protocols with a low CTDI value were used for the measurements with X-ray films. The Gafchromic films were used with a high additional dose and CTDI value imaging protocols, in a solid water phantom, with repeated acquisitions conducted without film movement or change.

Beam profile analysis

We investigated the effect of the half-bowtie filter on the shape of the beam. The effect of varying the energy on the beam profile width was investigated by using different imaging protocols (Head low dose, Breast, Head, Thorax, Pelvis — Tab. 1). A PTW 23332 rigid stem ionization chamber was used to perform relative measurements with a sensitive volume of 0.3 cm^3. The chamber was placed in a solid-water phantom insert at a depth of 20 mm above an 80 mm backscattering layer. Planar imaging was performed with the kilovoltage source at maximum field size (2300 × 2300 mm^2). Beam profile points were detected in four main perpendicular directions of the field in a plane parallel to the accelerator ring using 5–10 mm steps, starting the chamber from the isocenter.

The change of beam width was examined in the lateral position as the periphery position of the CTDI phantom. This is the result of the lateral movement centre of the detector array out from the imaging and the LINAC isocenter. Thorax imaging protocol was used with multiple beam widths (20–120 mm). The detector matrix was moved 70 mm and 150 mm from the isocenter in four directions in a plane and parallel to the accelerator ring.

CTDI

Based on the following equation, to determine the acquisition dose of a CT, the CT dose index i.e. CTDI dosimetric parameter can be used:

$$CTDI_{100} = \frac{1}{N \cdot T} \int_{-50}^{50} D(z)dz$$

In the definition, D(z) is a z-axis dose profile perpendicular to the tomographic plane, it is a line integrated dose value along the sensitive volume of the detector. The denominator (N·T) is equal to the number of detector pixels activated during imaging (N) and their nominal width (T) due to the International Standard [18].

A correction has to be applied for large beam widths (more than 40 mm) for the CBCTs, which is calculated using the following relation:

$$CTDI_{100,(N\cdot T)>40} = CTDI_{w,100,ref} \cdot \frac{CTDI_{FA,N\cdot T}}{CTDI_{FA,ref}}$$

where and are determined by using small beam widths (less than 40 mm), which was the reference beam width (ref). The values were measured in free air by using a wide (N·T) and a reference beam width as defined by the IAEA (19,20). Thus, two beam widths are used simultaneously in the determination of CTDI values of the CBCT protocols.

The CTDI measurements were performed with a Radcal 10X6-3CT pencil ionization chamber (Radcal, Monrovia, CA, USA) with a sensitive volume of 100 mm. The chamber determines the integrated dose value of a given dose profile along a line; therefore, the displayed value of the Radcal

Accu-Gold Touch detector has mGy·cm dimension, projected to 10 mm. Data were collected in air and in the PureImaging CTDI phantom (Pure Imaging Phantoms, Spring Court, Farnham Royal, UK). The phantom material is poly(methyl methacrylate) (PMMA), which consists of two parts. Its core is a block of 160 mm in diameter and 145 mm in length, which represents the head of an adult human (Fig. 2B). This is surrounded by the other part of the phantom in a ring, which has a total diameter of 320 mm and represents the human body (Fig. 2A). The central part of the phantom has five and the outer annular part has four more holes equally spaced, where the ionisation chamber can be inserted during measurements.

Dose-length product and effective dose values

The additional dose to patients during acquisition can be characterised by the effective dose. The effective dose can be used to estimate stochastic side effects [21]. The effective dose was determined from the measurements using the following relationship:

$$E = CTDI_{100,(N\cdot T)>40} \cdot N \cdot T \cdot k = DLP \cdot k$$

where E is the effective dose, DLP is the dose-length product and k is a weighting factor which depends only upon body regions, is the large beam width corrected CTDI value, N is the number of detector pixels activated during imaging and T is their nominal width [22]. In our study, k-factors were taken from the NRPB-W67 reference, because these values were defined with the CT phantom that we also used [23].

Results

Since the vendor-based FOV parameters were the most closely related to the measured beam widths, our measurement results were compared to these values displayed on the linear accelerator console.

Uncertainty of field size adjustment

Discrepancies were found in the field size adjustment related to the opening direction of the collimators. For a given field size setting, different beam width values were measured depending on whether the FOV was reduced or increased because two different Range values connected to one FOV, with a difference of 1 mm. The maximum deviation was 0.55 ± 0.02 mm for a FOV of 80 mm. The different profiles with 70 mm and 71 mm Range parameters for 80 mm FOV are illustrated in Figure 3. FOV's were investigated from 10 to 200 mm range, and the average of the setup uncertainties was 0.3 ± 0.02 mm (Tab. 2).

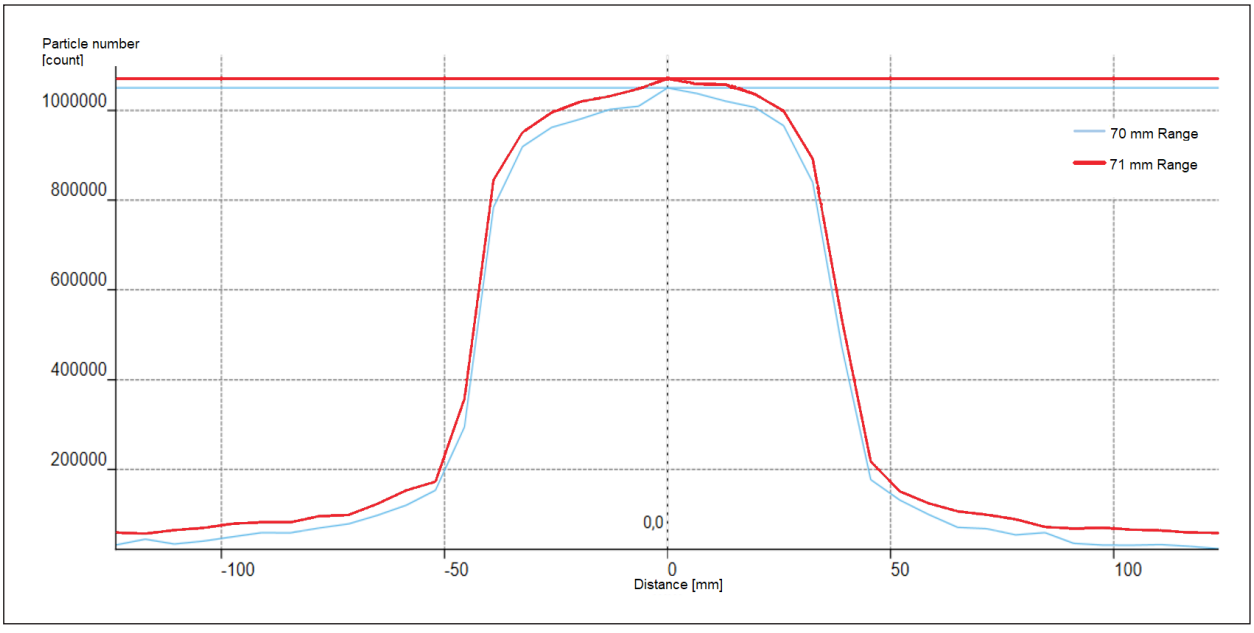

Figure 3. Comparison of beam profiles at 80 mm field of view (FOV) for 70 mm and 71 mm reconstructed image (Range) parameters

Energy dependence of the beam profiles

The influence of energy on beam profiles was investigated by measuring the width of the beam for each imaging protocols using a fixed field size. The maximum standard deviation of the beam widths detected for the 20 mm field size for the different imaging protocols was 0.45 ± 0.03 mm. For smaller FOVs (smaller than 20 mm), the standard deviations of the measured beam widths were between 0.13–0.25 mm (Tab. 3).

Dependence of beam width on field size

The dependence of the beam width on the field size was investigated by using two different ionization chamber detector matrices (Tab. 4). We used the same Thorax imaging protocol for all our measurements.

With the different ionisation chamber detector matrices, the same results were obtained considering the measurement accuracy of the instruments. The largest discrepancies occurred for small field sizes, which play a significant role in determining the CTDI values of kV CBCT. The results also show that the measured beam width is larger than the expected parameter for FOV of up to 110 mm. However, this is reversed for FOVs of 120 mm and larger field sizes; smaller beam widths were detected than expected based on the field size. Using the Wilcoxon Signed-Rank test, there is a significant difference between the manufacturer's FOV parameters and the measured beam widths, with a p-value of 0.00164.

Beam profile analysis

The variation of measured beam width was comparable to the measurement error, so the width of the integral of the swept areas was nearly constant as the source rotates around the circular orbit. However, for different field sizes, smaller beam widths were measured for the right-hand offsets than for the left-hand ones, standing opposite the linear accelerator. For upward and downward shifts, symmetric differences were observed from the isocenter.

Therefore, the beam profile was investigated in large open-field planar mappings by scanning the beam in two dimensions using relative measurements with a rigid ionization chamber. The results are shown in Figure 4.

The measurements show that the gradient of the left side of the beam is steeper than the right side (Fig. 4A). This phenomenon is the result of the half-bowtie filter, whose beamforming effect was detected for the kV CBCT mounted on the Ethos linear accelerator. In the case of upward and downward deflections, i.e. the vertical beam profile, symmetrical results were obtained (Fig. 4B).

CTDI

Based on the beam width parameters corrected by our measurements, the CTDI values were recalculated and compared with our previous publication results and the vendor-based data [24]. To measure and calculate the CTDI values, we used the method explained in this publication, corrected for large beam width. The wide beam width of the CBCT was 200 mm but to determine the CTDI a reference beam width of 10 mm FOV was used, which is consistent with the recommendations for the CTDI determination of CBCTs [20, 25].

Table 4. Dependence of beam width on field size for a given imaging protocol

FOV [mm]	Measured_IBA [mm]	Measured_PTW [mm]	Deviation_IBA-FOV [mm]	Deviation_PTW-FOV [mm]
10	14.2 ± 0.15	12.6 ± 0.46	4.17 ± 0.15	2.6 ± 0.46
20	21.4 ± 0.12	21.4 ± 0.21	1.43 ± 0.12	1.43 ± 0.21
40	41.1 ± 0.2	40.7 ± 0.2	1.1 ± 0.2	0.8 ± 0.2
60	60.4 ± 0.06	60.5 ± 0.26	0.43 ± 0.06	0.47 ± 0.26
80	80.7 ± 0.12	80.7 ± 0.21	0.73 ± 0.12	0.7 ± 0.21
100	100.9 ± 0.15		0.87 ± 0.15	
110	110.2 ± 0.14		0.2 ± 0.14	
120	119.3 ± 0.17		-0.7 ± 0.17	
160	159.6 ± 0.35		-0.43 ± 0.35	
200	198.4 ± 0.15		-0.57 ± 0.15	

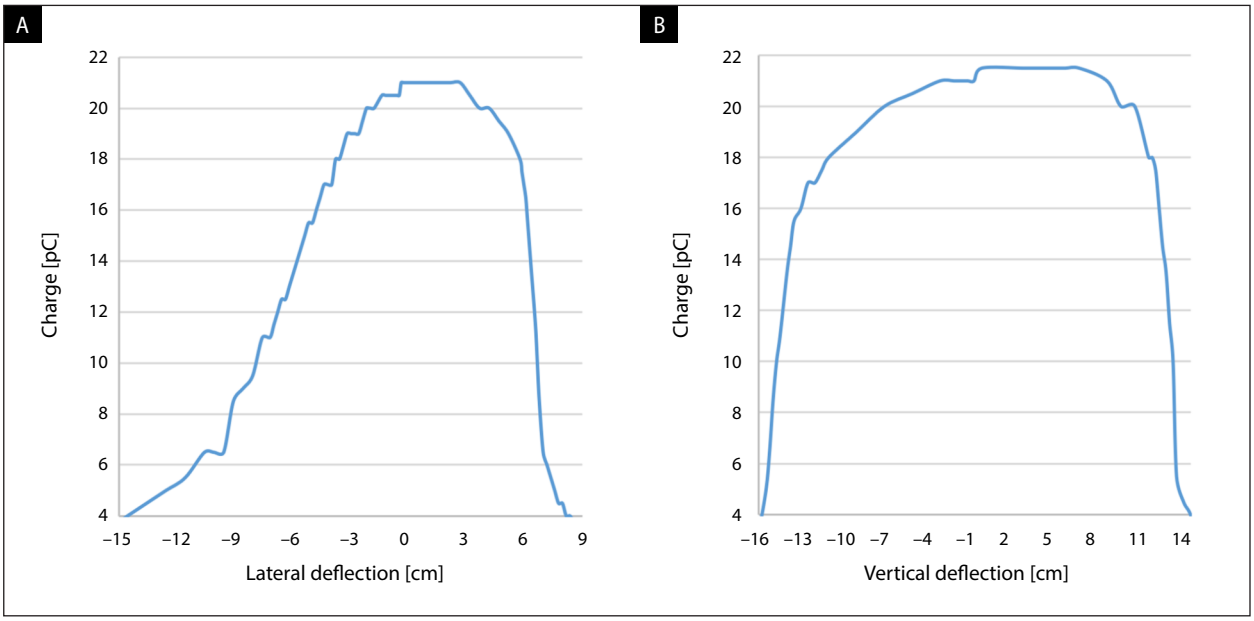

Figure 4. Shape of two-dimensional PTW 23222 rigid stem ionisation chamber scanned cone beam computed tomography (CBCT) beam profile

The smallest relative deviation from the vendor-based data was 2.3 % (0.5 mGy) for the pelvis imaging protocol. For breast imaging protocol, we found the largest relative deviation of 12.2 % (0.12 mGy) (Tab. 5). Detected values were higher than the vendor-based values for all imaging protocols. By reducing the reference beam width and correcting the beam widths, CTDI values were detected higher than previously measured with a reference beam width of 17 mm (Fig. 5) [24].

DLP and effective dose values

The DLP and effective dose values recorded during the acquisition phase exceeded the values specified by the manufacturer for all imaging protocols (Tab. 6). The lowest discrepancies were observed for the pelvic imaging protocol, as evidenced by the CTDI values. With regard to the percentage deviation, the maximum value was 11.5% for the breast.

Discussion

The radiographic film is often used for the verifications of field size [26]. Gonzalez-Lopez, et al. used radiochromic films in their study about small fields due to high spatial resolution [27]. Jurkovic et al. the dosimetry of scattered, low energy photons with radiographic film [28]. Based on our investigation, in some cases, the X-ray film was overexposed and a plateau was obtained during the evaluation, which made it impossible to determine the half-width of the profile. In other cases, widening due to scattered radiation became unmanageable. Prentou et al. used EBT3 radiochromic film in kV X-ray radiation therapy study [29]. The dose of CBCT exposure did not cause polymerization in EBT3, even when the imaging protocol with the highest additional dose was repeatedly applied in the same setup. The EBT3 film was used for our study due to its ability to detect a wide range of radiation doses, from 0.1 cGy to 10 Gy, and energy-independence, as per the manufacturer's instructions. A suitable measurement setup for film dosimetry was not found using the tools available.

The ionisation chamber detector matrices can be used to perform various patient-specific and linear accelerator quality assurance tests. The major advantages of detector matrices are the reusability and real-time monitoring over film dosimetry. Ritter et al. published a study about the meaningful and efficient linear accelerator commissioning or monitoring with 2D detector array [30]. Anvar et al. compared the usability of 2D Matrixx and radiochromic film for the quality assurance of photon beams and observed a good agreement [31]. M. Liebmann et al. used a two-dimensional detector array for CT and cone-beam CT dosimetry [32].

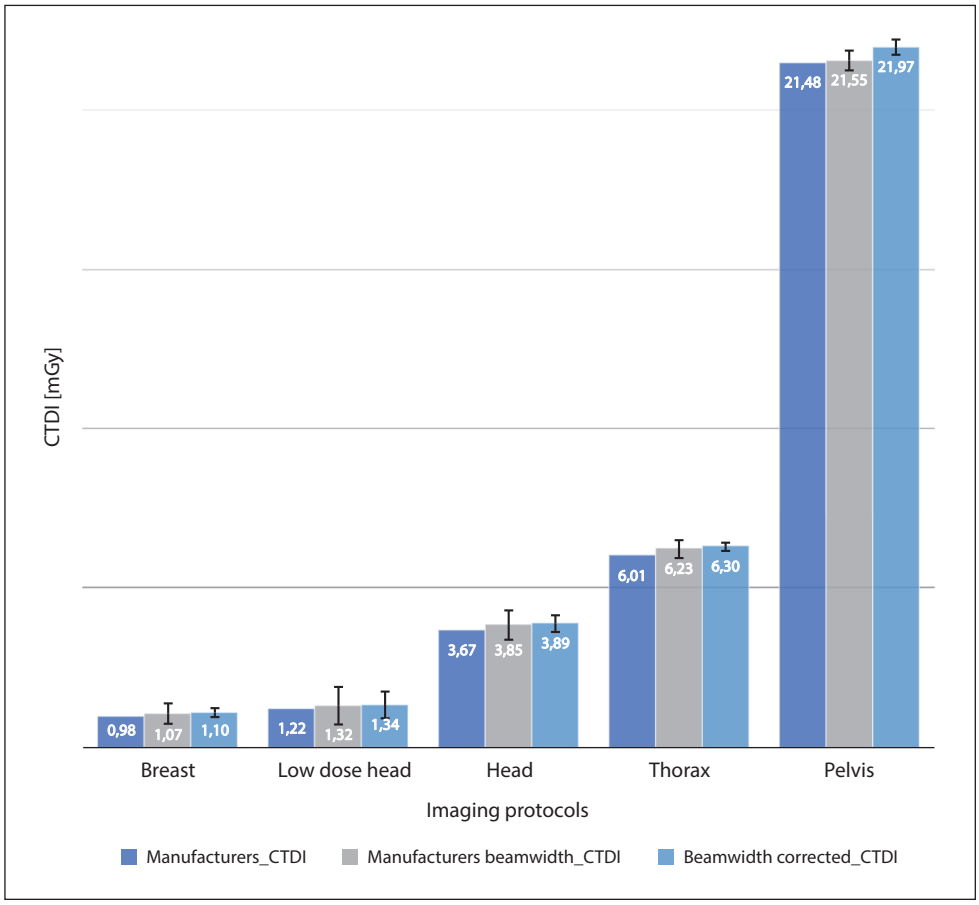

Figure 5. Comparison of the computed tomography dose index (CTDI) values with and without beam width correction and the vendor-based values based on the different cone beam computed tomography (CBCT) imaging protocols

Table 6. Comparison of dose length product (DLP) and effective dose values, calculated from computed tomography dose index (CTDI) as estimated by the manufacturer and corrected for measured beam width

Protocols	Manufacturers_DLP [mGy· mm]	Expected_E [mSv]	Beam width corrected_ DLP [mGy· mm]	Beam width corrected_E [mSv]
Head	734	0.169	772.6 ± 1.3	0.178 ± 0.13
Head low dose	245	0.056	266.1 ± 2.4	0.061 ± 0.24
Thorax	1203.8	2.046	1251.2 ± 4.2	2.127 ± 0.42
Breast	196	0.333	218.5 ± 1.4	0.371 ± 0.14
Pelvis	4298	8.166	4363.2 ± 12.6	8.290 ± 1.26

In our study small beam widths were measured using PTW Octavius 1000 SRS, while beam widths exceeding 80 mm FOV were measured using IBA Matrixx Resolution ionization chamber detector matrix. Comparing data detected at the same field sizes, the two systems gave identical results, except for FOV below 20 mm.

Kim and Alaei implemented the full and half bowtie models of kV CBCT in a treatment planning system [33]. During the validation process they show the dose distribution of kV static X-ray beam with half bowtie filter geometry in a cubic water phantom. A similar dose distribution was detected by the semiflexible ionization detector chamber based on our investigation.

There are no sources in the international literature to describe the manufacturer's definition of the CTDI for CBCT, and the manufacturer does not define the field size parameter that describes the beam width at the isocenter of the linear accel-

erator. The predicted CTDI values of imaging protocols increase in direct proportion to the growth of the tube current parameter.

The CTDI values corrected by the measured beam width were higher than those specified by the manufacturer for all imaging protocols. Henceforth, the measured doses during the imaging process were underestimated, because of the detection efficiency [25]. Thus, the effective dose of imaging is much higher than the vendor-based data.

The magnitude of the discrepancies did not appear to be large; however, these results are for one acquisition and the effective dose has to be multiplied by the number of CBCTs connected to the therapy session. For the effective dose, it should be noted that the mathematical formula used to calculate it contains hypothetical concepts and expressions involving large uncertainties in the causal relations between radiation dose and stochastic effects and is not able to predict the future risk of cancer for any organ or tissue. Therefore, it cannot be used for estimating individual or population cancer risk and cannot be used as a basis for epidemiological studies. However, it is an appropriate general measure for determining radiation protection dose limits [21].

Conclusions

The measured CTDI coefficient calculated with the measured beam width was higher than predicted by the manufacturer for each imaging protocol; however, during the measurements, the effect of every parameter could not be considered, for example; scattered dose, uncertainty of detectors, setup errors, etc. The results of our measurements show that while the smallest relative difference of CTDI values was detected for the pelvis protocol, this causes the largest absolute difference in effective dose.

The currently internationally recommended CTDI measurement protocols for CBCT do not contain reference to the determination of the beam width as a basic element of the calculations. Based on our measurement results, the beam width parameters affect CTDI, therefore it would be advisable to apply this type of correction.

Conflict of interests

The authors declare that they have no known competing financial interests or personal relationships that could have appeared to influence the work reported in this paper.

Sz.G-H. and Á.G. designed the study, Sz.G-H. performed the experiments, Sz.G-H. analysed the data and wrote the article in consultation with Cs.P. and T.M. The tests were done with the help of G.S., D.Sz. and E.K.

Funding

The project was implemented with support from the National Research, Development and Innovation Fund of the Ministry of Culture and Innovation under the National Laboratories Program (National Tumor Biology Laboratory (2022-2.1.1-NL-2022-00010)) Grant Agreement with the National Research, Development and Innovation Office.

References

1. Alaei P, Spezi E. Imaging dose from cone beam computed tomography in radiation therapy. Phys Med. 2015; 31(7): 647–658, doi: 10.1016/j.ejmp.2015.06.003, indexed in Pubmed: 26148865.
2. Pramanik S, Ray D, Bera S, et al. Analysis of setup uncertainties and determine the variation of the clinical target volume (CTV) to planning target volume (PTV) margin for various tumor sites treated with three-dimensional IGRT couch using KV-CBCT. J Radiat Oncol. 2020; 9(1–2): 25–35, doi: 10.1007/s13566-020-00417-z.
3. Liang J, Li M, Zhang T, et al. The effect of image-guided radiation therapy on the margin between the clinical target volume and planning target volume in lung cancer. J Med Radiat Sci. 2014; 61(1): 30–37, doi: 10.1002/jmrs.42, indexed in Pubmed: 26229633.
4. Dang HQ, Nguyen CT, Pham HV, et al. The institutional experience of the implementing 4DCT in NSCLC radiotherapy planning. Rep Pract Oncol Radiother. 2023; 28(4): 445–453, doi: 10.5603/RPOR.a2023.0056, indexed in Pubmed: 37795228.
5. Peng J, Li H, Laugeman E, et al. Long-term Inter-protocol kV CBCT image quality assessment for a ring-gantry linac via automated QA approach. Biomed Phys Eng Express. 2020; 6(1): 015025, doi: 10.1088/2057-1976/ab693a, indexed in Pubmed: 33438613.
6. Pathak PK, Vashisht SK, Baby S, et al. Commissioning and quality assurance of Halcyon 2.0 linear accelerator. Rep Pract Oncol Radiother. 2021; 26(3): 433–444, doi: 10.5603/RPOR.a2021.0065, indexed in Pubmed: 34277097.
7. Altergot A, Schürmann M, Jungert T, et al. Imaging doses for different CBCT protocols on the Halcyon 3.0 linear accelerator - TLD measurements in an anthropomorphic phantom. Z Med Phys. 2024; 34(4): 580–595, doi: 10.1016/j.zemedi.2023.03.002, indexed in Pubmed: 37088675.
8. Dracham CB, Shankar A, Madan R. Radiation induced secondary malignancies: a review article. Radiat Oncol J. 2018; 36(2): 85–94, doi: 10.3857/roj.2018.00290, indexed in Pubmed: 29983028.

9. Dzierma Y, Mikulla K, Richter P, et al. Imaging dose and secondary cancer risk in image-guided radiotherapy of pediatric patients. Radiat Oncol. 2018; 13(1): 168, doi: 10.1186/s13014-018-1109-8, indexed in Pubmed: 30185206.
10. Kibrom AZ, Knight KA. Adaptive radiation therapy for bladder cancer: a review of adaptive techniques used in clinical practice. J Med Radiat Sci. 2015; 62(4): 277–285, doi: 10.1002/jmrs.129, indexed in Pubmed: 27512574.
11. Åström LM, Behrens CP, Calmels L, et al. Online adaptive radiotherapy of urinary bladder cancer with full re-optimization to the anatomy of the day: Initial experience and dosimetric benefits. Radiother Oncol. 2022; 171: 37–42, doi: 10.1016/j.radonc.2022.03.014, indexed in Pubmed: 35358605.
12. Vañó E, Miller CJ, Rehani MM et al. Diagnostic Reference Levels in Medical Imaging. ICRP Publication 135. Ann. ICRP 46(1). https://www.icrp.org/publication.asp?id=icrp%20publication%20135.
13. IAEA. Safety Reports Series No. 21: Optimization of Radiation Protection in the Control of Occupational Exposure. IAEA Safety Rep. 2002: 65.
14. Casar B, Lopes Md, Drljević A, et al. Medical physics in Europe following recommendations of the International Atomic Energy Agency. Radiol Oncol. 2016; 50(1): 64–72, doi: 10.1515/raon-2016-0004, indexed in Pubmed: 27069451.
15. Gáldi Á, Farkas G, Gazdag-Hegyesi S, et al. Combined biological effects of CBCT and therapeutic X-ray dose on chromosomal aberrations of lymphocytes. Radiat Oncol. 2024; 19(1): 109, doi: 10.1186/s13014-024-02504-8, indexed in Pubmed: 39143640.
16. Liu F, Yang Q, Cong W, et al. Dynamic bowtie filter for cone-beam/multi-slice CT. PLoS One. 2014; 9(7): e103054, doi: 10.1371/journal.pone.0103054, indexed in Pubmed: 25051067.
17. Mutic S, Palta JR, Butker EK, et al. AAPM Radiation Therapy Committee Task Group No. 66. Quality assurance for computed-tomography simulators and the computed-tomography-simulation process: report of the AAPM Radiation Therapy Committee Task Group No. 66. Med Phys. 2003; 30(10): 2762–2792, doi: 10.1118/1.1609271, indexed in Pubmed: 14596315.
18. International Standard Norme Internationale. Medical electrical equipment — Part 2–44: Particular requirements for the basic safety and essential performance of X-ray equipment for computed tomography Appareils électromédicaux — Partie 2–44: Exigences particul. 2009. www.iec.ch/searchpub/cur_fut-f.htm (06.06.2023).
19. Winkler NT. Quality Control in Diagnostic Radiology. SPIE Semin Proc. 1975; 70: 125–131.
20. IAEA TECREPO-5. Status of Computed Tomography Dosimetry for Wide Cone Beam Scanners. IAEA 2011: 1–55.
21. Fisher DR, Fahey FH. Appropriate Use of Effective Dose in Radiation Protection and Risk Assessment. Health Phys. 2017; 113(2): 102–109, doi: 10.1097/HP.0000000000000674, indexed in Pubmed: 28658055.
22. Collins L. Comments on the 1990 Recommendations of the International Commission on Radiological Protection — ICRP publication 60. South Afr Med J. 1992; 81(11): 583–6.
23. Shrimpton PC, Hillier MC, Lewis MA, et al. Doses from Computed Tomography (CT) Examinations in the UK — 2003 Review. Natl Radiol Prot Board. 2005; 57(March): 1–107. http://www.biophysicssite.com/Documents/NRPB_W67/NRPB_W67.pdf.
24. Gazdag-Hegyesi S, Gáldi Á, Major T, et al. Dose indices of kilovoltage cone beam computed tomography for various image guided radiotherapy protocols. Radiat Prot Dosimetry. 2023; 199(8-9): 983–988, doi: 10.1093/rpd/ncad101, indexed in Pubmed: 37225198.
25. Boone JM. The trouble with CTD100. Med Phys. 2007; 34(4): 1364–1371, doi: 10.1118/1.2713240, indexed in Pubmed: 17500467.
26. Botwin K, Ceraulo P, Shah C. Radiation Safety for the Physician. Pain Proced Clin Pract. 2011: 31–36, doi: 10.1016/b978-1-4160-3779-8.10005-3.
27. Gonzalez-Lopez A, Vera-Sanchez JA, Lago-Martin JD. Small fields measurements with radiochromic films. J Med Phys. 2015; 40(2): 61–67, doi: 10.4103/0971-6203.158667, indexed in Pubmed: 26170551.
28. Jurkovic S, Zauhar G, Faj D, et al. Dosimetric verification of compensated beams using radiographic film. Radiol Oncol. 2011; 45(4): 310–314, doi: 10.2478/v10019-011-0020-9, indexed in Pubmed: 22933972.
29. Prentou E, Papagiannis P, Pantelis E, et al. [OA153] EBT3 radiochromic film dosimetry in kV X-ray radiation therapy. Phys Med. 2018; 52: 58–59, doi: 10.1016/j.ejmp.2018.06.225.
30. Ritter TA, Gallagher I, Roberson PL. Using a 2D detector array for meaningful and efficient linear accelerator beam property validations. J Appl Clin Med Phys. 2014; 15(6): 4749, doi: 10.1120/jacmp.v15i6.4749, indexed in Pubmed: 25493506.
31. Varasteh Anvar M, Attili A, Ciocca M, et al. Quality assurance of carbon ion and proton beams: A feasibility study for using the 2D MatriXX detector. Phys Med. 2016; 32(6): 831–837, doi: 10.1016/j.ejmp.2016.05.058, indexed in Pubmed: 27246359.
32. Liebmann M, Poppe B, von Boetticher H. Computed tomography dosimetry with high-resolution detectors commonly used in radiotherapy - an energy dependence study. J Appl Clin Med Phys. 2015; 16(5): 396–407, doi: 10.1120/jacmp.v16i5.5302, indexed in Pubmed: 26699294.
33. Kim S, Alaei P. Implementation of full/half bowtie filter models in a commercial treatment planning system for kilovoltage cone-beam CT dose estimations. J Appl Clin Med Phys. 2016; 17(2): 153–164, doi: 10.1120/jacmp.v17i2.5988, indexed in Pubmed: 27074480.